ELSEVIER

Chemical Engineering Journal 74 (1999) 217–223

Chemical Engineering Journal

Short communication

Numerical prediction of the liquid flow within a hydrocyclone

G.Q. Dai*, J.M. Li, W.M. Chen

Department of Hydraulic Engineering, Sichuan University, Chengdu 610065, China

Received 11 August 1997; received in revised form 7 July 1998; accepted 31 January 1999

Abstract

The three-dimensional flow fields with a central air core in a hydrocyclone are numerically simulated using a k–ε turbulence model. The model constants C_1, C_2 and C_μ are modified because of the anisotropic character of the turbulent viscosity in the hydrocyclone. Experiments show that the predicted velocity profiles agree well with data measured by laser Doppler anemometry (LDA). Based on this prediction, the flow field and the pressure field as well as the distribution of the rate of dissipation of the turbulent energy are discussed. The study shows that an important approach towards reducing energy dissipation in a hydrocyclone is to improve the flow pattern in the cylindrical part.

Keywords: Hydrocyclone; Turbulence; Numerical simulation; Flow field

1. Introduction

As a simple, easy to operate and effective solid–liquid separation apparatus, the hydrocyclone has been applied widely in the chemical, metallurgical and petroleum industries. Hydrocyclones have usually been designed on the basis of empirical equations to determine their geometric and operating parameters. However, because of the wide number of applications and better operational requirements for hydrocyclones, it is becoming apparent that the design of a hydrocyclone using empirical or semi-empirical equations has many limitations. In addition, model experiments can consume much time and entail much cost. Several investigators [1–7] have studied the fluid flow within a hydrocyclone by numerical simulation in order to reveal the separation mechanism and to determine the total efficiency and the grade efficiency. In this paper, the turbulent flow of the liquid phase in a hydrocyclone is simulated by employing the k–ε turbulence model whose constants had to be partly revised on the basis of the experimental data measured by laser Doppler anemometry (LDA). The results predicted for the velocity fields and the pressure fields may provide an important basis for the design and the operation of a hydrocyclone.

2. Mathematical model

2.1. Basic equations

The liquid flow within a hydrocyclone is a three-dimensional helical movement with a free surface (air core). So, an accurate description of the flow must include a set of three-dimensional elliptic equations, i.e. the Navier–Stokes equations. On the basis of turbulence theory [8], the k–ε model was selected as the computational model because analytical solutions for Navier–Stokes equations are usually impossible. It was verified form the measurements obtained by Hsieh and Rajamani [4] that the flow within a hydrocyclone is axisymmetric except for that in the inlet part. So, the governing equation in a cylindrical coordinate system is expressed as

$$\frac{\partial}{\partial x}(\rho r u\Phi)+\frac{\partial}{\partial r}(\rho r v\Phi)=\frac{\partial}{\partial x}\left(\Gamma_\Phi r\frac{\partial\Phi}{\partial r}\right)+\frac{\partial}{\partial r}\left(\Gamma_\Phi r\frac{\partial\Phi}{\partial r}\right)+rS_\Phi$$

Eq. (1) is a partial differential equation in common use where Φ represents different variables, Γ_Φ a diffusion coefficient and S_Φ a source term. For the various values of Φ, Γ_Φ and S_Φ have corresponding meanings, as shown in Table 1.

$$\mu_e=\mu+\mu_t;\quad \mu_t=\frac{C_\mu\rho k^2}{\varepsilon};$$

*Corresponding author. E-mail: dgql@mail.sc.cninfo.net

1385-8947/99/$ – see front matter
PII: S1385-8947(99)00044-3

Table 1
The variables in the partial differential Eq. (1)

Equation	Φ	Γ_Φ	S_Φ
Continuity	1	0	0
Momentum	u	μ_e	$-\frac{\partial \rho}{\partial x}+\frac{\partial}{\partial x}\left(\mu_e \frac{\partial u}{\partial x}\right)+\frac{1}{r}\frac{\partial}{\partial r}\left(r\mu_e \frac{\partial v}{\partial x}\right)$
	v	μ_e	$-\frac{\partial \rho}{\partial r}+\frac{1}{r}\frac{\partial}{\partial r}\left(r\mu_e \frac{\partial v}{\partial r}\right)+\frac{\partial}{\partial x}\left(\mu_e \frac{\partial v}{\partial r}\right)-\frac{2\mu_e \nu}{r^2}+\frac{\rho w^2}{r}$
	w	μ_e	$-\frac{\mu_e w}{r^2}+\frac{\rho v w}{r}-\frac{w}{r}\frac{\partial \mu_e}{\partial r}$
Turbulent kinetic energy	k	μ_e/σ_k	$G-\rho\varepsilon$
Energy dissipation rate	ε	μ_e/σ_ε	$\frac{\varepsilon}{k}(C_1 G - C_2 \rho\varepsilon)$

$$G=\mu_t\left\{2\left[\left(\frac{\partial u}{\partial x}\right)^2+\left(\frac{\partial v}{\partial r}\right)^2+\left(\frac{v}{r}\right)^2\right]+\left(\frac{\partial u}{\partial r}+\frac{\partial v}{\partial x}\right)^2+\left[\left(\frac{\partial w}{\partial x}\right)^2+\left(\frac{\partial w}{\partial r}-\frac{w}{r}\right)^2\right]\right\} \quad (2)$$

For the classical k–ε model, the usual values for the constants in the above equations are: $C_\mu = 0.09$, $C_1 = 1.44$, $C_2 = 1.92$, $\sigma_k = 1.0$, and $\sigma_\varepsilon = 1.3$. However, these constants could not be used to simulate the turbulent flow within a hydrocyclone because the results of Xu et al. [9] show that the turbulent flow in a hydrocyclone is strongly anisotropic. The axial relative turbulence is the strongest of the three-dimensional velocities. So, the corresponding eddy viscosity coefficient may be relatively different. Our study [10] shows that the turbulent flow in a hydrocyclone is strongly anisotropic. The corresponding eddy viscosity coefficient can be written as follows:

$$\mu_{e,ij} = \mu + \mu_{t,ij} \quad (3)$$

where

$$\mu_{t,ij} = \frac{C_{\mu,ij}\rho k^2}{\varepsilon}; \quad ij = ux, ur, vx, vr, wx, w\theta;$$

$$C_{\mu,ij} = \begin{bmatrix} C_{\mu,ux} & C_{\mu,ur} & C_{\mu,u\theta} \\ C_{\mu,vx} & C_{\mu,vr} & C_{\mu,v\theta} \\ C_{\mu,wx} & C_{\mu,wr} & C_{\mu,w\theta} \end{bmatrix} = \begin{bmatrix} \frac{2}{3}C_\mu & \frac{1}{3}C_\mu & \frac{2}{3}C_\mu \\ \frac{1}{3}C_\mu & \frac{1}{3}C_\mu & C_{\mu,v\theta} \\ \frac{2}{3}C_\mu & C_{\mu,wr} & \frac{1}{3}C_\mu \end{bmatrix} \quad (4)$$

wherein $C_{\mu,wr}$ is equal to $C_{\mu,v\theta}$, which could not be expressed simply as a constant times C_μ. However, stress in an azimuthal direction can be described by the following formula [5]:

$$\mu_{t,wr} = \mu_{t,v\theta} = \rho(l_{r\theta} r)^2 \left[\left(\frac{\partial u}{\partial r}\right)^2+\left(r\frac{\partial}{\partial r}\frac{w}{r}\right)^2\right]^{1/2} \quad (5)$$

2.2. Modification to model constants

A preliminary computation showed that there were large differences between the simulated results obtained by the standard k–ε model and the measured values. The main reason is that the standard k–ε model is based on an isotropic turbulence assumption. Some researchers have recently improved the model by using an anisotropic eddy viscosity to reduce the deviation of the calculation [11]. However, 10 new coefficients have to be determined from the experimental results. Thus the development of an anisotropic model implies complicated equations and cannot be commonly used. Therefore, in this paper, some constants of the standard k–ε model will be modified in order to improve the computational accuracy.

The constants C_1 and C_2 in the standard k–ε model were determined from experimental data measured in a wind tunnel with almost uniform velocity fields. These constants have also been used for liquid flows in pipes. However, it is apparent that the constants C_1 and C_2 determined in this way are not adaptable to the situation wherein there is a large velocity gradient in a hydrocyclone. It can be seen from the physical meanings of the terms in the ε equation that C_1 is proportional to the turbulence generation term and C_2 is proportional to the turbulence dissipation rate. The generation term should be enlarged or the dissipation term reduced, i.e. C_1 should be increased or C_2 decreased, in order to make the calculated results possess the characteristics of high velocity gradients and strong turbulence in a hydrocyclone. Otherwise, a uniform velocity distribution will result if the generation term is less than the dissipation term or the dissipation term is greater than the generation term. In other words, the flows in a hydrocyclone would not remain turbulent if the generation term is less than the dissipation term.

There are certain ways for modifying the model constants [7,12]. By simply modifying the model constants, it is possible to overcome the problem successfully and to save computational time. The authors' measurements showed that the results would be good if C_1 was increased, and C_2 and C_μ were decreased. After some trials $C_1 = 1.62$, $C_2 = 1.79$ and $C_\mu = 0.085$ were chosen. Fig. 2 shows that the predicted profiles of the axial velocity agree well with the values measured by two-component LDA.

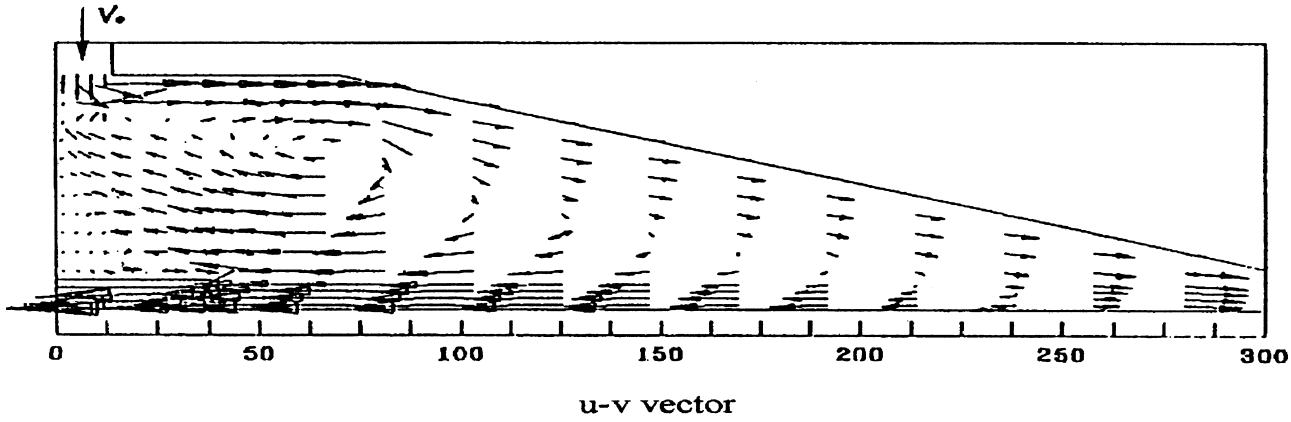

Fig. 1. u–v vector plot.

3. Calculation example

The diameter of the hydrocyclone was 80 mm, the cone angle 15°, the length of the cylindrical part 70 mm, the length of the conical part 250 mm, the diameter of the tangential inlet 14 mm and the diameters of the underflow orifice and the vortex finder were both 14 mm. The inlet pressures were 3×10^4, 6×10^4 and 9×10^4 Pa. The diameter of the air core under these conditions remains constant and was 8.5 mm as per the experimental result [13]. The inlet velocity of the liquid was determined by mass conservation conditions, i.e.

$$u_0 = 0, \quad v_0 = \frac{Q_{\text{in}}}{(\pi D_c d_{\text{in}})}, \quad w_0 = \frac{4Q_{\text{in}}}{\pi(d^2_{\text{in}})}$$

The variables of the control volume near the walls were modified using the 'wall-function method'. Around the free surface (air core)

$$v = \frac{\partial u}{\partial r} = \frac{\partial w}{\partial r} = \frac{\partial k}{\partial r} = \frac{\partial \varepsilon}{\partial r} = 0$$

and at fluid exit planes

$$v = \frac{\partial u}{\partial x} = \frac{\partial w}{\partial x} = \frac{\partial k}{\partial x} = \frac{\partial \varepsilon}{\partial x} = 0$$

There were 27 (axial) × 17 (radial) grid nodes in the area for computation. The numerical calculation method was the same as that used in the literature [14], i.e. the equations were solved using the SIMPLER computer code. The relative residual of the velocity components was 1.0×10^{-3}, and that of k and ε was 5.0×10^{-2}. The number of iterations was 3994.

4. Results and discussion

4.1. Velocity fields

Fig. 1 shows a vector plot in the axisymmetric plane of the hydrocyclone, i.e. the distribution plots of the resultant of the axial velocity and the radial velocity. Fig. 2 shows the profiles of the axial velocity. Fig. 3 shows the profiles of the tangential velocity. Fig. 4 shows a plot of the radial distribution of the radial velocity under the condition of an inlet

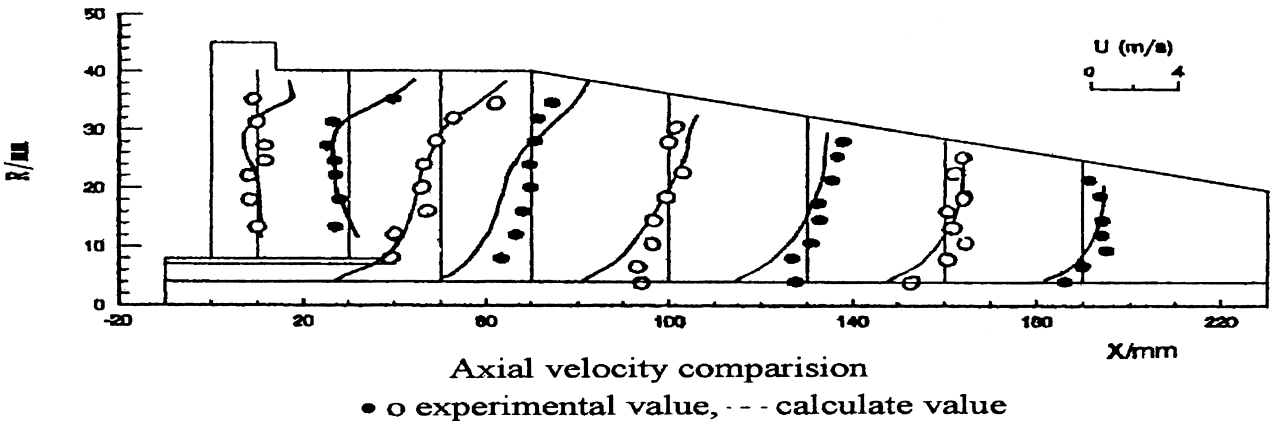

Fig. 2. Axial velocity comparison: ●, ○, experimental; ———, calculated.

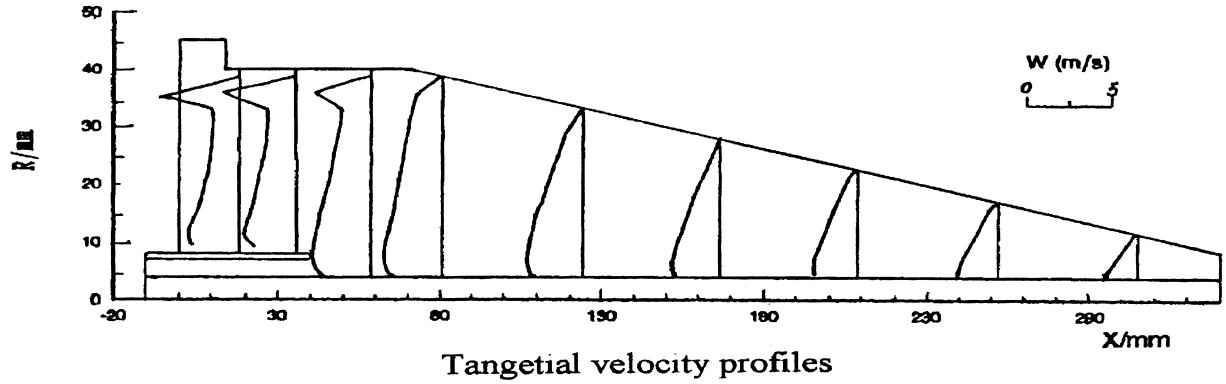

Fig. 3. Tangential velocity profiles.

pressure of 6×10^4 Pa. It is clear from Fig. 1 that there is a recirculating movement of the liquid in the cylindrical and upper parts of the cone. At the same time, a small secondary eddy is generated near the outer wall of the vortex finder. This eddy makes it possible for a small amount of liquid to move along the top wall of the hydrocyclone, then down the outer wall of the vortex finder, and finally into the overflow, thus forming the so-called 'short-circuit' flow. The bulk flow of liquid moves helically down the inner wall of the cone and leaves through the underflow orifice in the apex of the cone. In the cone part, some of the liquid reverses its flow direction and moves up, forming the inner helical flow. Some of the liquid in the inner helical flow will recirculate in the totoridal region, while the rest would go out through the vortex finder. The velocity distribution obtained in this article agrees well with Davidson's computational result [15]. In his article, Rhodes's expression [3] of the eddy viscosity coefficient was used to modify the Prandtl mixing-length model. Fig. 2 shows that the maximum axial velocity occurs near the air core. The axial velocity is relatively small between the outer wall of the vortex finder and the inner wall of the cylindrical part. The large discrepancy between the measured and the computed values near the air-core is due to the inaccurate measurement of the axial velocity resulting from the unstable displacement of the air-core. It is shown in Fig. 3 that the radial distribution of the tangential velocity in the cylindrical part has a two-peak shape. One peak velocity is near the air core, and the other is at the inlet of the hydrocyclone. The reason for this is that there exists a strong swirl flow at the inlet, while the peak tangential velocity near the air core results from the sharp decrease in the radial velocity and the pressure energy in this zone. Fig. 4 shows the radial velocity profiles in the hydrocyclone. It can be seen from Fig. 4 that the radial velocity component within the cone part decreases with decreasing radius.

4.2. Pressure distributions

Fig. 5 shows a pressure profile of the longitudinal half-part of the hydrocyclone. The inlet pressure is 6×10^4 Pa. It can be seen from Fig. 5 that the pressure decreases gradually from the inlet to the spigot and the vortex finder. For the same cross-section, the pressure is greatest at the hydrocyclone wall, and it decreases, first gently and then sharply near the air core. The minimum pressure occurs at the surface of the air core, and from the computations, it should be possible to determine whether the gauge pressure is less than zero at the surface of the air core.

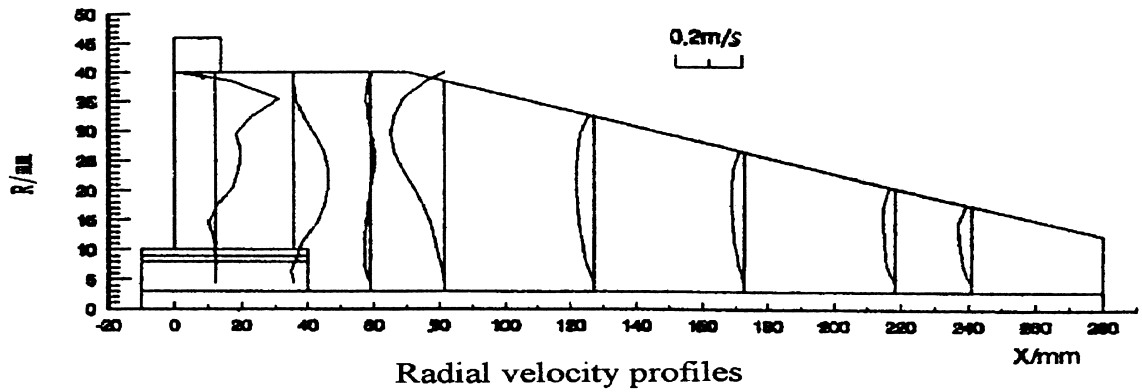

Fig. 4. Radial velocity profiles.

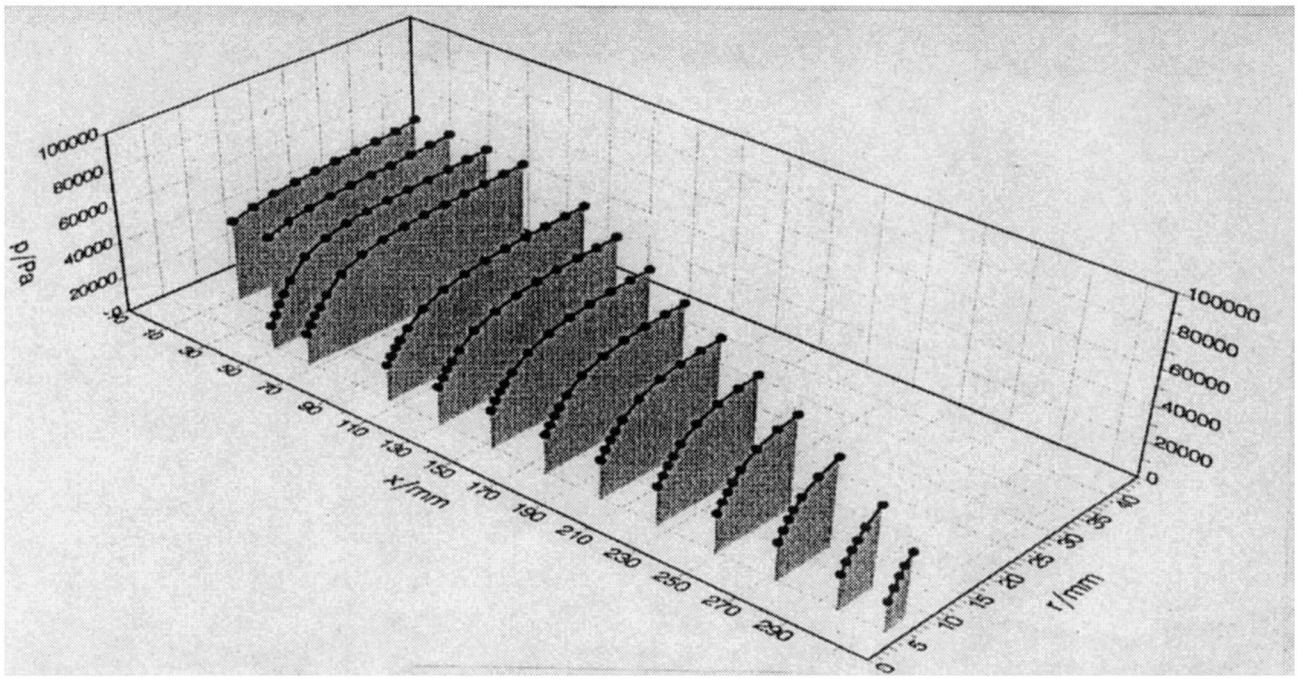

Fig. 5. Pressure distribution.

4.3. Dissipation rate of turbulent kinetic energy

The profiles of the turbulent energy dissipation rate in the hydrocyclone are shown in Fig. 6. Fig. 7 shows that the kinetic energy profiles are similar to those of the dissipation rate. The larger values of the dissipation rate occur in the zone near the entrance to the vortex finder, as do those of the kinetic energy. It is found in this zone that the flow pattern is very complicated, the eddies generate and dissipate violently, and the turbulence is very strong. It is shown that the turbulent kinetic energy and its dissipation rate in the hydrocyclone depend closely upon changes in the flow pattern. The flow pattern in the cylindrical part should

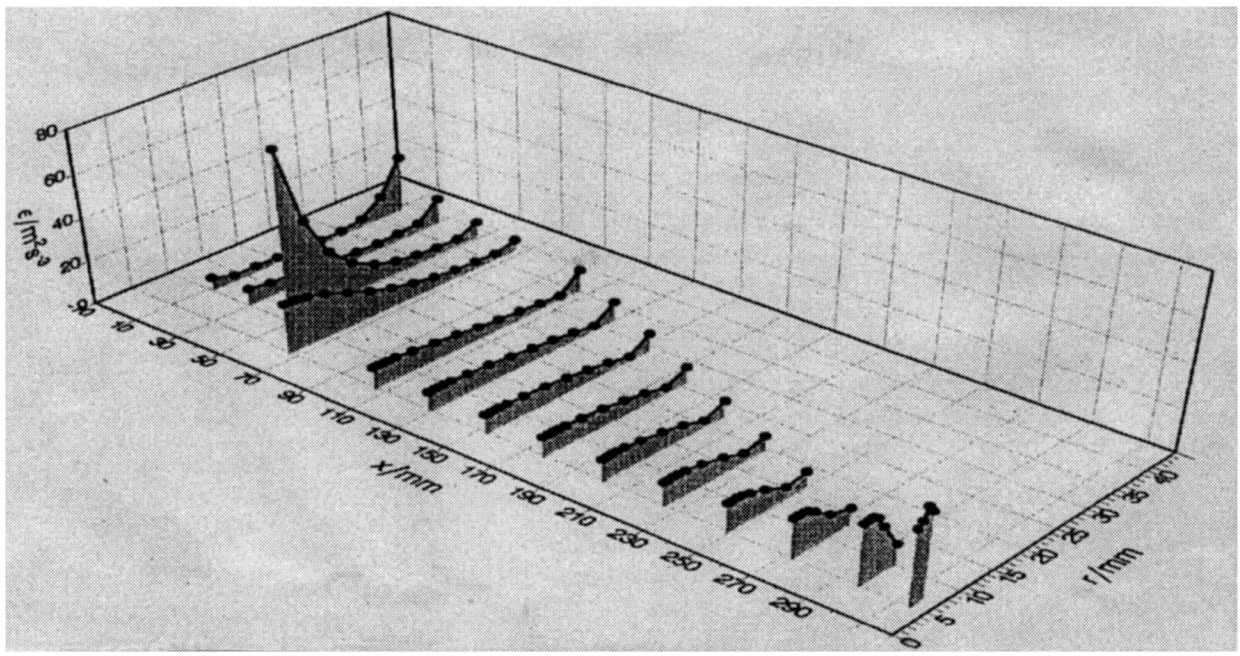

Fig. 6. Distribution of turbulent energy dissipation rate.

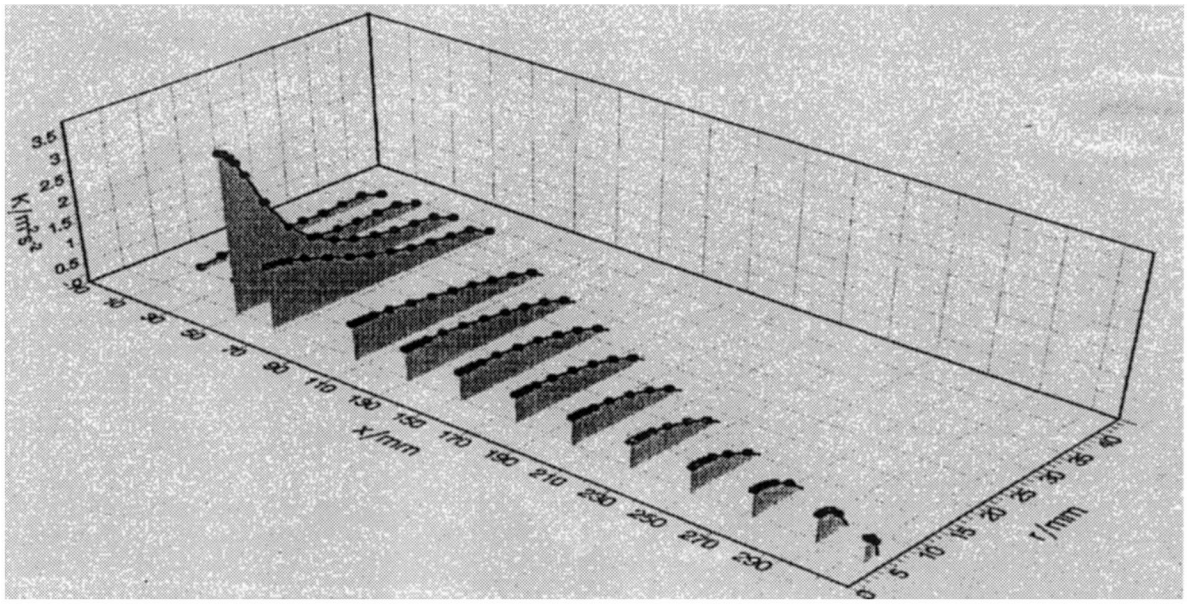

Fig. 7. Distribution of turbulent energy.

be improved in order to reduce the energy dissipation in a hydrocyclone.

5. Conclusions

The modified k–ε model presented in this article can be used to predict the velocity profiles in a hydrocyclone. The numerical predictions of the axial velocity profiles agree well with the experimental data.

The flows in a hydrocyclone are discussed in detail based on the computational results. One of the main ways to reduce the energy dissipation in a hydrocyclone is to improve the flow pattern in cylindrical part of a hydrocyclone.

The results of this study provide an important basis for further research on the separation mechanism and the optimal design of a hydrocyclone.

6. Nomenclature

C_1 constant of the turbulence model
C_2 constant of the turbulence model
C_μ constant of the turbulence model
d_{in} diameter of inlet pipe (m)
k turbulence ($m^2\ s^{-2}$)
p pressure (Pa)
Q_{in} inlet flow rate ($m^3\ s^{-1}$)
r radius (m)
r_{in} radius of inlet pipe ($m\ s^{-1}$)
u axial velocity component ($m\ s^{-1}$)
v radial velocity component ($m\ s^{-1}$)
x axial distance (m)
w tangential velocity component ($m\ s^{-1}$)

Greek letters

$\Gamma_{\Phi x}$ diffusion coefficient of Φ along x direction
$\Gamma_{\Phi r}$ diffusion coefficient of Φ along r direction
ε turbulence dissipation rate ($m^2\ s^{-3}$)
μ liquid viscosity (Pa s)
μ_e total viscosity (Pa s)
μ_t eddy viscosity (Pa s)
ρ liquid density ($kg\ m^{-3}$)
σ_ε constant of turbulence model
σ_k constant of turbulence model
Φ general variable

Subscript

0 inlet

Acknowledgements

This project was supported by the National Science Foundation of China (Project No. 29376225).

References

[1] M.I.G. Bloor, D.B. Ingham, Trans. I. Chem. Eng. 53 (1975) 1–6.
[2] K.R. Upadrashta, V.J. Ketcham, J.D. Miller, Int. J. Miner. Process 20 (1987) 309–318.

[3] N. Rhodes, K.A. Pericieous, S.N. Drake, in: Proc. 3rd Int. Conf. on Hydrocyclones, Oxford, England, 1987, pp. 51–58.
[4] K.T. Hsieh, R.K. Rajamani, Int. J. Miner. Process 22 (1988) 223–227.
[5] K.T. Hsieh, R.K. Rajamani, AIChE J. 37 (1991) 735–746.
[6] R.K. Duggins, P.C.W. Frith, Filtration and Separation 24 (1987) 394–397.
[7] T. Dyakowski, R.A. Williams, Chem. Eng. Sci. 48 (1993) 1143–1152.
[8] S.V. Patankar, Numerical Heat Transfer and Fluid Flow, McGraw-Hill, New York, USA (Maidenhead, UK), p. 1980.
[9] J. Xu, Q. Loc, J. Qiu, Filtration and Separation 27 (1990) 356–359.
[10] J.M. Li, G.Q. Dai, W.M. Chen, in: Proc. on Computational Hydraulics (in Chinese), Chengdu University of Science and Technology Press, Chengdu, 1996, pp. 231–237.
[11] S.Y. Ju, T.M. Mulabill, R.W. Pike, Trans. J. Chem. Eng. 68 (1990) 3–16.
[12] A. Melhotra, R.M.R. Branion, E.G. Hauptman, Can. J. Chem. Eng. 72 (1994) 953–960.
[13] R. Guo, M.E. Thesis, Sichuan Union University, Chengdu, 1996, pp. 15–33.
[14] G.Q. Dai, Ph.D. Thesis, Sichuan Union University, Chengdu, 1994, pp. 12–23.
[15] M.R. Davidson, Appl. Math. Modelling 12 (1988) 119–128.